PAPER REF: 4675

AA6082-T6 FRICTION STIR WELDED BUTT JOINTS OPTIMIZATION

Ana C. F. Silva[1(*)], Daniel F. O. Braga[1], M. A. V. de Figueiredo[2], P. M. G. P. Moreira[1]

[1]Institute of Mechanical Engineering and Industrial Management (INEGI), University of Porto, Porto, Portugal
[2]Department of Mechanical Engineering (DEMec), University of Porto, Portugal
[(*)]*Email:* asilva@inegi.up.pt

ABSTRACT

This paper presents an optimization study of friction stir welded joints (FSW) through the Taguchi and Artificial Neural Network methods. At the moment, there is a lack of FSW parameters optimization studies in the literature, which this study aims at addressing. Optimum parameters are of prime importance for future investigations, as it will allow for consistent and sound welds. This is of even greater relevance for industrial applications, as for FSW to become a mainstream joining technology, repeatability of good quality welds are key. The most influent welding parameters and their trends were identified. The process optimization for this alloy and tools was achieved and the best parameters combination to accomplished quality weld joint were selected.

Keywords: butt joints, Friction stir welding, optimization, Taguchi.

INTRODUCTION

Friction stir welding (FSW) is a highly reliable joining process capable of creating excellent opportunities for new structural design concepts for several industries, like aeronautic, aerospace and railway. It is a solid state welding process where a special tool is inserted in rotation between the workpieces edges and transversed along the line of the joint. The tool generates heat by friction and induces strong plastic deformation in the material, promoting its complex mixing across the joint (see in Fig. 1). This process is able to produce high quality joints. The ability to weld different types of materials, such as aluminum, magnesium, steels, titanium and others, as well as the possibility of creating dissimilar joints with excellent mechanical characteristics (surpassing other joining processes), adds to the interest in their study [1-4].

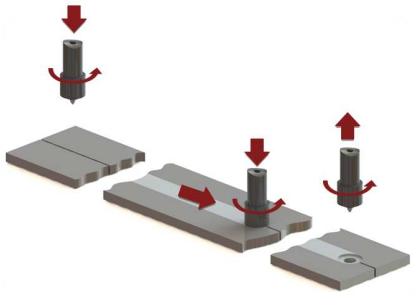

Fig. 1 - Schematic diagram of the FSW process.

One of the advantages of FSW technique, compared with the traditional fusion welding techniques is that the temperatures achieved are below the melting temperature of the materials to be joined, avoiding defects, such as porosity, and phase transformations. Low distortion, excellent mechanical properties in the weld zone, manufacturing without shielding gas, and suitability to weld all aluminum alloys, are also among the process advantages [3, 5]. This process was originally developed at The Welding Institute (TWI) for aluminum alloys, but since then FSW has been gradually implemented in joints of a large number of diferent materials, and even dissimilar joints have been produced with this technique [5].

Taguchi method is one of the most innovative methods for quality control that has been widely applied for optimization of materials processing. This method is based on the statistical analysis of data and offers a simple mean of analysis and optimization of complex systems. The Taguchi method proposes two ways of data analysis in order to determine optimum levels of control parameters and their influence in the process: analysis of variance (ANOVA) and signal to noise (S/N) ratio. In this work the ANOVA method was used.

Already, some Taguchi method applications for optimization of the friction stir welding process, may be found in the literature. In Lakshminarayanan [3] and Jayaraman [6], Taguchi method was applied to FS aluminum welds tensile properties, demonstrating that the rotational speed was the highest influential factor (more influential than welding speed and axial force). Similar studies for different alloys, investigating temperature achieved in welding and HAZ distances, achieved similar conclusions Nourani [2]. Other works of FSW process optimization are cited [1, 7-9].

METHODS AND MATERIAL

The welds were produced in 380x150x3 mm plates of aluminum AA6082-T6, along the rolling direction (see Fig. 2). A modified milling machine was used to perform the welds. The parameters selected to optimize and the values of each parameter are presented in Table 1. The probe profile and diameter (probe/shoulder ratio was defined by variation of the shoulder diameter) were maintained constant. The probe used has a 6 mm diameter, and a conical shape with a 0.5 mm step and four flutes. The shoulder has a concave shape. The tools geometry are shown in Fig. 3.

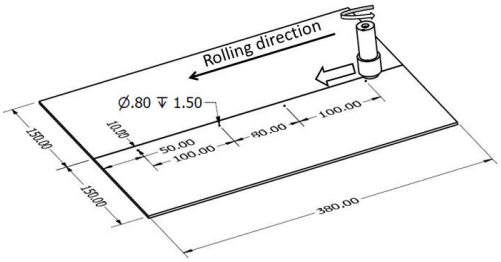

Fig. 2 - Welding test configuration and thermocouple location during welding.

Table 1 – Levels of the selected parameters.

Parameters		Unit	Level 1	Level 2	Level 3
A	Tool rotational speed	rpm	735	1000	1500
B	Welding speed	mm/min	216	290	360
C	Tilt angle	º	0	1	2
D	Probe distance from the root surface	mm	0.10	0.15	0.20
E	Shoulder/Probe diameters ratio (D/d)	-	2 (12/6)	2.5 (15/6)	3 (18/6)

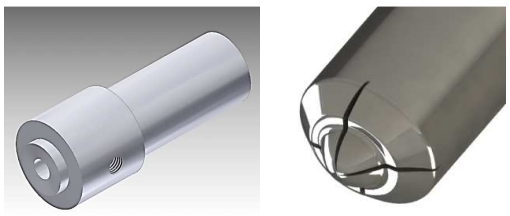

Fig. 3 - Pin and shoulder geometry.

To perform the experimental trials, the columns 1, 2, 6, 7, and 8 were chosen from the Taguchi L27 orthogonal array (OA). Three levels of each parameter were selected to define the combinations of parameters to perform the FSW experiments (see Table 1). The OA for the experiment and the corresponding table with the respective parameters values is presented in Table 2, where each line corresponds to a single test sample. Therefore 27 different butt joints were produced accordingly to the table.

Table 2 – Taguchi orthogonal array apply to the experiment. In the left are presented the columns of the L27 OA and in the right are present the correspondent parameters values.

Test	OA columns					Parameters				
	1	2	6	7	8	Rotational speed [rpm]	Welding speed [mm/min]	Tilt angle [^{0}]	Probe distance from the root surface [mm]	Shoulder/ probe ratio (D/d)
	A	B	C	D	E	A	B	C	D	E
1	1	1	1	1	1	735	216	0	0.10	2.00
2	1	1	2	2	2	735	216	1	0.15	2.50
3	1	1	3	3	3	735	216	2	0.20	3.00
4	1	2	1	1	2	735	290	0	0.10	2.50
5	1	2	2	2	3	735	290	1	0.15	3.00
6	1	2	3	3	1	735	290	2	0.20	2.00
7	1	3	1	1	3	735	360	0	0.10	3.00
8	1	3	2	2	1	735	360	1	0.15	2.00
9	1	3	3	3	2	735	360	2	0.20	2.50
10	2	1	2	3	1	1000	216	1	0.20	2.00
11	2	1	3	1	2	1000	216	2	0.10	2.50
12	2	1	1	2	3	1000	216	0	0.15	3.00
13	2	2	2	3	2	1000	290	1	0.20	2.50
14	2	2	3	1	3	1000	290	2	0.10	3.00
15	2	2	1	2	1	1000	290	0	0.15	2.00
16	2	3	2	3	3	1000	360	1	0.20	3.00
17	2	3	3	1	1	1000	360	2	0.10	2.00
18	2	3	1	2	2	1000	360	0	0.15	2.50
19	3	1	3	2	1	1500	216	2	0.15	2.00
20	3	1	1	3	2	1500	216	0	0.20	2.50
21	3	1	2	1	3	1500	216	1	0.10	3.00
22	3	2	3	2	2	1500	290	2	0.15	2.50
23	3	2	1	3	3	1500	290	0	0.20	3.00
24	3	2	2	1	1	1500	290	1	0.10	2.00
25	3	3	3	2	3	1500	360	2	0.15	3.00
26	3	3	1	3	1	1500	360	0	0.20	2.00
27	3	3	2	1	2	1500	360	1	0.10	2.50

The temperature was measured on the shoulder boundaries during welding process, using four thermocouples at the surface. Of the measured temperature results, only the highest values were considered. After welding, mechanical tests were performed, including tensile and bending tests as well as hardness profile determinations Tensile tests specimens extracted transversally to the weld line were performed according to ASTM E8-M [10]. These tests were performed using specimens with a reduce section length of 60 mm and 12.5 mm width. Bending tests were performed taking into consideration the NP EN 910 standard [11], with 160x20x3 mm specimens. This type of tests are very sensitive to defects such as root flaws.

These properties were then used in an ANOVA analysis with a 95 % confidence level. Mean main effect plot, response surface and regression analyses were also performed.

In the ANOVA analysis was not only studied each parameter effect on the properties but also three parameters interactions. These were as follows: tool rotational speed with welding speed (A*B), tool rotational speed with shoulder/Probe diameters ratio (D/d) (A*E) and welding speed with shoulder/probe diameters ratio (B*E). With these analysis it was possible to determine the most influential parameters, and their interactions, as well as trends in the analysed properties.

The mean main effect plot and response surface analyses possibilities obtain the trends of each factor in the properties. With the regression analysis it is possible to obtain an equation to predict the properties of the joint for each factor analysed.

RESULTS AND DISCUTION

The results of the measurements performed are presented in Table 4.

Exploring previous analysis it may be seen that temperatures between 189 and 474 ºC, respectively, were achieved. Xu [12], reported temperatures in the order of magnitude of 500 ºC during the welding process. In the studied alloy, the main strengthening precipitate is β”-Mg_5Si_6 which is stable at temperatures lower than 200 ºC, and during welding, the β” is easily dissolved, corrupting properties joint [2, 7, 13, 14].

Observing the tensile test results, 76 % and 60 % tensile and yield strengths efficiencies (ratio between obtained properties and base metal properties), were verified (see Table 3). Similar values were achieved in other studies [4, 7, 14].

Table 3 - Mechanical properties of AA6082-T6 aluminium alloy, base material [14].

Property	Value
Tensile strength (MPa)	322.9
Yield strength (MPa)	276.2
Elongation (%)	17.5

Concerning the hardness profiles, a decrease in the thermo mechanically affected zone (TMAZ) and a significant variation on its size with increase of shoulder diameter (from 5.7 mm to a 21.0 mm), were observed. Some typical hardness profiles of joints obtained with each shoulder diameter are presented in Fig. 4. Also, it was verified that the weld hardness minimum values are obtained in the welding retreating side, varying 56.6-72.8 HV and in some cases showing a decrease of almost 50% when compared to the base material. This type of profile was also observed in previous studies [4, 14, 15].

Table 4 – Results obtained for each parameters combination.

Test	Temperature [º]	Tensile properties			Hardness profile	Bending properties
		Tensile [MPa]	$Yield_{0.2\,\%}$ [MPa]	Elongation [%]	TMAZs size [mm]	Max Load [N]
1	189	210	146	3.8	5.7	580
2	366	233	154	5.6	12.6	826
3	459	231	149	5.3	19.2	648
4	429	207	143	3.7	15.6	341
5	474	189	156	2.6	17.1	341
6	359	213	150	3.6	9.9	428
7	403	148	135	2.2	9.9	255
8	331	199	155	2.9	9.6	357
9	363	208	156	3.1	11.7	585
10	385	235	160	4.2	11.1	442
11	434	205	132	3.8	17.1	256
12	429	231	151	6.0	15.6	605
13	369	243	160	6.2	14.4	851
14	432	203	143	3.1	20.4	428
15	362	244	160	6.4	10.2	673
16	358	142	141	1.4	18.6	203
17	413	241	161	4.5	10.2	590
18	325	246	166	4.7	9.6	543
19	281	238	157	6.0	14.4	826
20	363	230	152	4.3	13.5	364
21	453	188	154	1.9	18.6	321
22	328	183	157	2.4	16.5	384
23	450	225	143	5.2	21.0	4340
24	356	169	157	2.0	14.1	341
25	451	214	155	3.2	18.0	505
26	399	215	163	3.0	12.0	419
27	309	228	143	6.2	15.9	804

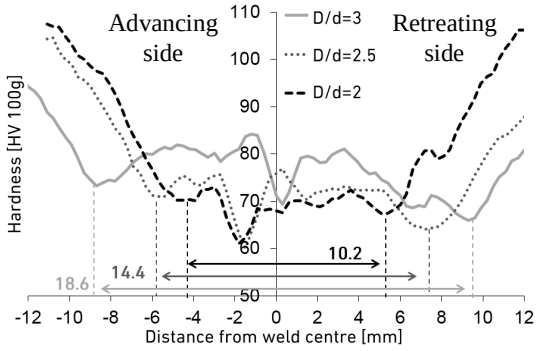

Fig. 4 - Typical hardness profile for the three diameters of shoulder/probe ratio with the correspondent mean for each diameter.

Analysis of variance considering a level of confidence of 95 %, were performed to study which parameters showed the highest influence in the different properties evaluated. The

contribution percentage obtained with these analysis is presented in Table 5. A significant residual error was obtained. However the results obtained were similar to those found in the literature, witch corroborates the results achieved in this work. Analysing the results, it was verified that the most influent parameter in the factors analysed was the shoulder/probe diameters ratio (D/d). It also may be seen that the effect of the two speeds and the shoulder diameter are dependent of each other in most of the analysis performed.

Table 5 – Parameters and interaction percentage contribution for the different properties analysed.

Parameter	Temperature	Tensile properties			Hardness profile	Bending properties
		Tensile	$Yield_{0,2\ \%}$	Elongation	TMAZs size	Max Load
A	0.2 %	5.3 %*	-	3.6 %*	10.2 %	-
B	1.9 %	5.2 %*	-	6.8 %*	3.3 %	0.02 %
C	0.6 %	4.3 %*	1.0 %	1.9 %	4.6 %	-
D	0.4 %	8.5 %*	1.7 %	5.3 %*	-	4.14 %
E	**38.8 %***	**14.3 %***	**5.1 %***	5.7 %*	**47.6 %***	5.5 %
A*B	9.5 %	**11.5 %***	2.6 %	**12.2 %***	-	**21.9 %***
A*E	**17.4 %***	7.9 %*	4.2 %	0.9 %	-	-
B*E	**18.5 %***	**14.8 %***	1.0 %	4.9 %*	-	5.9 %

*parameter with significance level bellow to 0.05.

The main effects of each parameter for each factor are presented in Fig. 5. Also estimated responses of the interactions are presented in surface and contour form in Fig. 6.

Observing the results for the rotational speed trends in the different analysed factors, it was observed that better joint quality was achieved with 1000 rpm, especially regarding tensile strength and elongation analyses. Elangovan [9] in a study to predict tensile properties of FSW Al6061 alloy described also an optimum rotational speed at 1200 rpm. This conclusion was justified by defects, like pinhole or cracks appearing when lower speeds were used. Nonetheless, the higher rotational speeds introduce longer defects, like tunnel, due to increase in turbulence. While regarding the increase of rotational speed, promoted higher temperatures leading to lower tensile properties [9, 16]. The tool rotational speed has influence in the TMAZ size, where its increase leads to an enlargement of the heat affected zone size, as the heat generated by friction is larger, also verified in [2].

Concerning welding speed it was shown that using higher welding speed, lower mechanical strength may be achieved, strongly supported by trends shown in ANOVA analysis of tensile strength and elongation. This fact can be related to the lower time that the material has to achieve the proper temperature for the plastic flow and may lead to defects formation, such as voids. This poor consolidation of the metal interface results in a week interface, this evidence is also verified in [2, 7, 9, 16].

Regarding the interaction between the rotational and welding speeds, it was shown, an increase of properties with the use of speeds proportionally grouped by the level. This may be confirmed in Fig. 6 where the response surface of the interaction between the welding speed (B) and the tool rotational speed (A), is presented. It was also, verified that the best welds may be achieved using both speeds in the medium level (1000 rpm and 290 mm/min).

The analysis of the tilt angle influence was not conclusive. For the probe distance to the root surface, the lower distance resulted in weakest mechanical properties and have a slight decrease at the highest distance (0.2 mm), which may be verified by the high significance in

tensile strength and elongation in ANOVA analysis. This may be due to the strong plastic deformation near the root surface, however an incomplete probe penetration can lead to root flaws. The best properties are obtained with a probe distance of 0.15 mm from the root surface, as shown in Fig. 5.

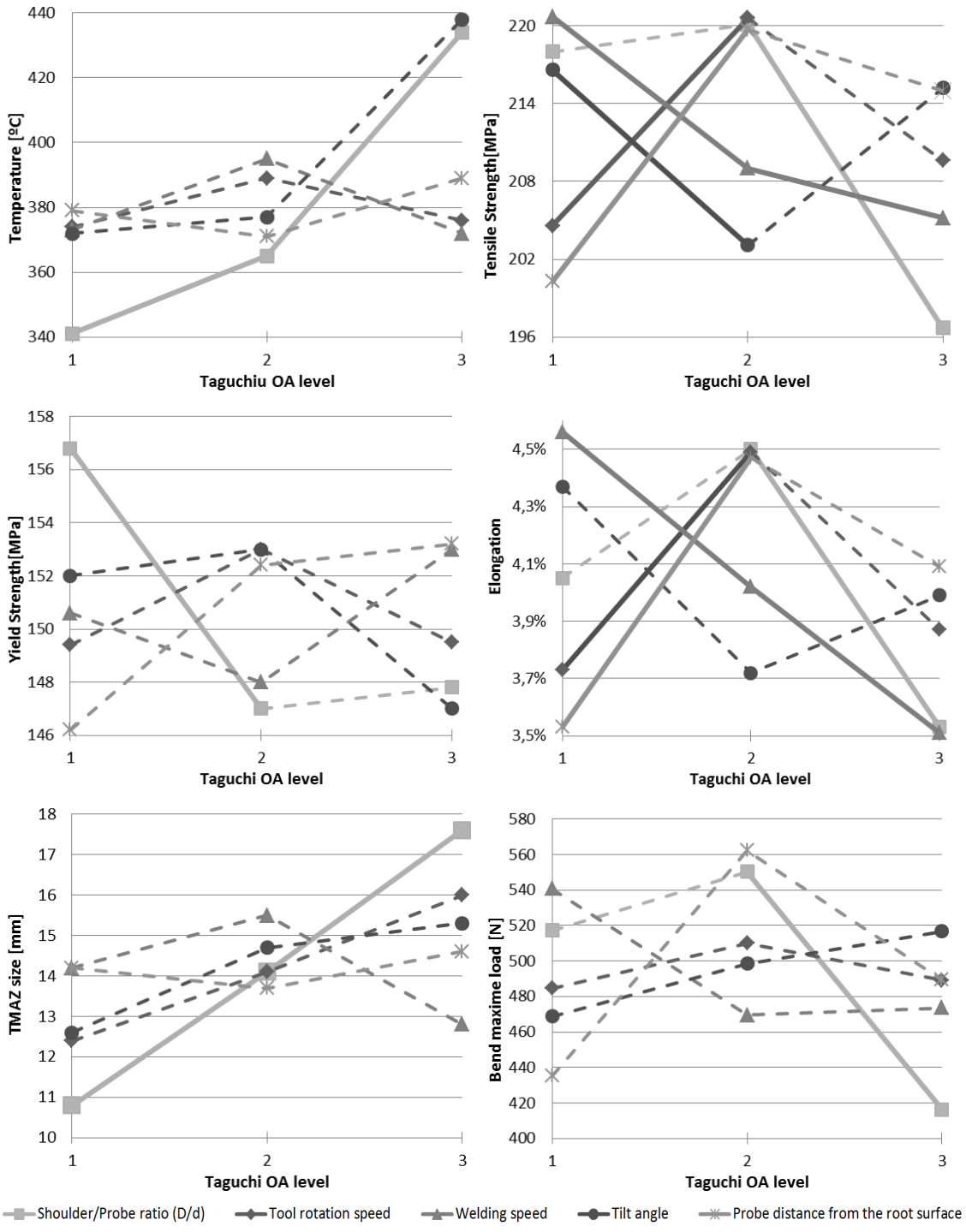

Fig. 5 – Main effect of the different parameters in the temperature and the properties analysed. The solid

line denotes the significant trends of each analysis obtain by Fisher method.

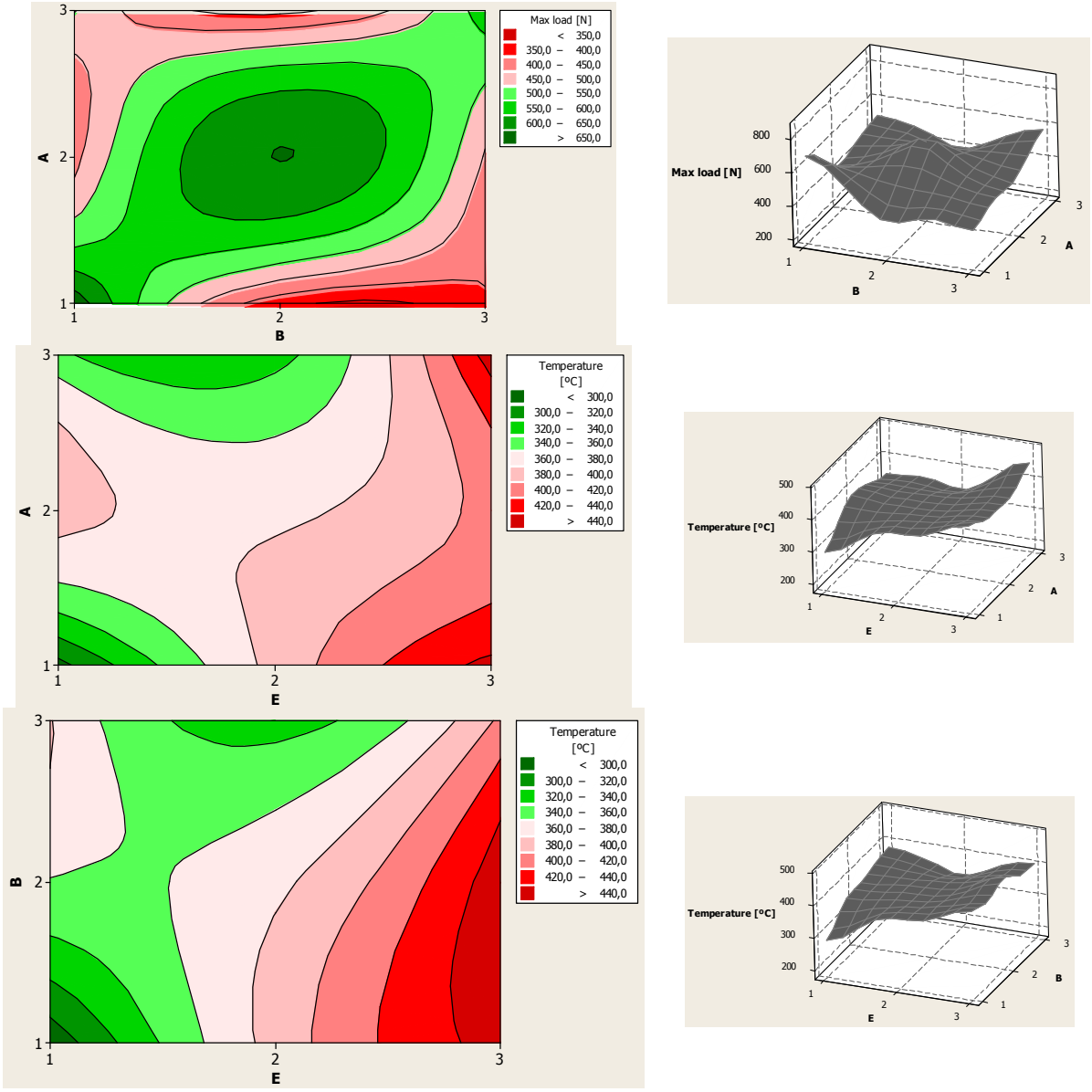

Fig. 6 – Contours plot and estimate response surface for the interactions analysis with most significance.

On the subject of the shoulder/probe diameters ratio it was observed that using higher shoulder diameter, provides weakest mechanical properties which corroborated in all ANOVA analyses (see Fig. 5). This is due to friction heat generated derivate from a larger area, in referred in Lertora [17]. Most of the heat is generated at the interface between the tool shoulder and the work-pieces [16].

In relation to the interactions speeds and the probe/shoulder diameters it was verified that the speeds effects are higher when smaller shoulder diameters are used. An increase of properties and lower temperatures are observed with the use of smaller shoulder diameters (see Fig. 6). In respect to the interaction between the tool rotational speed with the probe/shoulder diameters, it was verified that a combination of a lower tool rotation speed with a lower

diameter shoulder results in smaller TMAZ size, corresponding to smaller temperatures results. In interaction between welding speed and shoulder/probe diameters, it was observed that best welds were obtained when lower levels are used or increased welding speeds with medium level of the probe/shoulder diameter ratio.

The combination that gives improved joint mechanical properties, accordingly to the performed analysis, was: 1000 rpm with 290 mm/min, 0.15 mm pin distance to the root surface and a probe/shoulder diameters ratio of 2 (shoulder diameter of 12 mm).

From the regression analysis, several equations for joint optimization and prediction were obtained, presented in Table 6.

Table 6 - Equations with regression coefficients to estimate joints properties and estimated properties to improved joint.

	Equation
Temperature	27 – 0.0014 A – 0.003 B + 9.4 C + 97 D + 92.5 E
Tensile strength	272 + 0.00278 A – 0.108 B – 0.65 C + 147 D – 21.4 E
Yield strength	161 – 0.00068 A + 0.0172 B – 2.54 C + 70.4 D – 9.00 E
Elongation	0.0676-0.000000A-0.000073B-0.00188C+0.0556D-0.00527 E
TMAZs size	-7.15 + 0.00462 A – 0.00924 B + 1.35 C + 4.33 D + 6.80 E
Bend max load	783 – 0.0002 A – 0.472 B + 23.9 C + 513 D - 101 E

It is important to refer that this optimization was only performed for AA6082-T6 aluminium alloy and using the tool geometry presented in Fig. 3.

CONCLUSION

It was demonstrated that Taguchi's robust orthogonal array design method is suitable to analyze FSW joints. The ANOVA approach leaded to the contribution of each parameter and their interaction in the properties analysed.

The joints presented an efficiency of 76 % for the tensile and 60 % for yield strengths when compared with base material properties.

It was observed that the tools diameters ratio was the most influent factor in the joint quality and also that the weld speed, the tool rotational speed and the probe/shoulder diameters ratio are dependent on each other.

Improved joints may be achieved by using 1000 rpm with 290 mm/min, 0.15 mm from the probe to the root surface and a probe/shoulder diameters ratio of 2 (shoulder diameter of 12 mm).

ACKNOWLEDGMENTS

This work was supported by the FCT project PTDC/EME-TME/114703/2009 and FCT project PTDC/EME-TME/117596/2010. Dr. Moreira acknowledges POPH – QREN-Tipologia 4.2 – Promotion of scientific employment funded by the ESF and MCTES. The collaboration of Mr. José Almeida during the welding trials is gratefully acknowledged.

REFERENCES

1. Cavaliere, P., A. Squillace, and F. Panella, *Effect of welding parameters on mechanical and microstructural properties of AA6082 joints produced by friction stir welding.* Journal of Materials Processing Technology, 2008. **200**(1–3): p. 364-372.
2. Nourani, M., A.S. Milani, and S. Yannacopoulos, *Taguchi Optimization of Process Parameters in Friction Stir Welding of 6061 Aluminum Alloy: A Review and Case Study.* Engineering Failure Analysis, 2011. **3**: p. 144-155.
3. Lakshminarayanan, A.K. and V. Balasubramanian, *Process parameters optimization for friction stir welding of RDE-40 aluminium alloy using Taguchi technique.* Transactions of Nonferrous Metals Society of China, 2008. **18**(3): p. 548-554.
4. Moreira, P.M.G.P., M.A.V. de Figueiredo, and P.M.S.T. de Castro, *Fatigue behaviour of FSW and MIG weldments for two aluminium alloys.* Theoretical and Applied Fracture Mechanics, 2007. **48**(2): p. 169-177.
5. Moreira, P.M.G.P., et al., *Mechanical and metallurgical characterization of friction stir welding joints of AA6061-T6 with AA6082-T6.* Materials & Design, 2009. **30**(1): p. 180-187.
6. Jayaraman, M., et al., *Optimization of process parameters for friction stir welding of cast aluminium alloy A319 by Taguchi method.* Journal of Scientific & Industrial Research, 2009. **68**: p. 36-43.
7. Heidarzadeh, A., et al., *Tensile behavior of friction stir welded AA 6061-T4 aluminum alloy joints.* Materials & Design, 2012. **37**(0): p. 166-173.
8. Rajakumar, S., C. Muralidharan, and V. Balasubramanian, *Establishing empirical relationships to predict grain size and tensile strength of friction stir welded AA 6061-T6 aluminium alloy joints.* Transactions of Nonferrous Metals Society of China, 2010. **20**(10): p. 1863-1872.
9. Elangovan, K., V. Balasubramanian, and S. Babu, *Predicting tensile strength of friction stir welded AA6061 aluminium alloy joints by a mathematical model.* Materials & Design, 2009. **30**(1): p. 188-193.
10. *ASTM E8/E8M - 09 Standard Test Methods for Tension Testing of Metallic Materials*, 2009.
11. *NP EN 910 Ensaios destrutivos em soldadura de materiais metálicos. Ensaio de dobragem.*, 1999.
12. Xu, W., et al., *Influence of welding parameters and tool pin profile on microstructure and mechanical properties along the thickness in a friction stir welded aluminum alloy.* Materials & Design, 2013. **47**(0): p. 599-606.
13. Shang, B.C., et al., *Investigation of quench sensitivity and transformation kinetics during isothermal treatment in 6082 aluminum alloy.* Materials & Design, 2011. **32**(7): p. 3818-3822.
14. Moreira, P.M.G.P., V. Richter-Trummer, and P.M.S.T. Castro, *Fatigue Behaviour of FS, LB and MIG Welds of AA6061-T6 and AA6082-T6*, in *Multiscale Fatigue Crack Initiation and Propagation of Engineering Materials: Structural Integrity and Microstructural Worthiness*, G.C. Sih, Editor. 2008, Springer Netherlands. p. 85-111.
15. Lohwasser, D. and Z. Chen, *Friction Stir Welding - From Basics to Applications.* 2010: Woodhead Publishing.
16. Nandan, R., T. DebRoy, and H.K.D.H. Bhadeshia, *Recent advances in friction-stir welding – Process, weldment structure and properties.* Progress in Materials Science, 2008. **53**(6): p. 980-1023.

17. Lertora, E. and C. Gambaro, *AA8090 Al-Li Alloy FSW parameters to minimize defects and increase fatigue life*. International Journal of Material Forming, 2010. **3**(1): p. 1003-1006.